Microelectronics Reliability 85 (2018) 12–18

Contents lists available at ScienceDirect

Microelectronics Reliability

journal homepage: www.elsevier.com/locate/microrel

Effect of negative potential on the extent of PID degradation in photovoltaic power plant in a real operation mode

Josef Hylský*, Dávid Strachala, Petr Vyroubal, Pavel Čudek, Jiří Vaněk, Petr Vanýsek

Department of Electrical and Electronic Technology, Faculty of Electrical Engineering and Communication, Technická 10, 616 00 Brno, Czech Republic

A R T I C L E I N F O

Keywords:
Potential induced degradation
Negative voltage potential
Photovoltaic power plant
SolidWorks simulation
Photovoltaic modules

A B S T R A C T

This paper deals with Potential Induced Degradation (PID) of *p*-type monocrystalline PV modules (Evergreen) from a photovoltaic power plant that has been in operation mode for 7 years. Within the PV module affected by the PID degradation, the effect of the electric field on individual PV cells is studied. The distribution of the electric field was simulated by SolidWorks software. The results show a random distribution of affected PV cells not related to the size and distribution of the electric field intensity. Furthermore, the dependencies of negative voltage potential on the range of PID degradation of individual PV modules located in the negative pole of the PV string is made. From measured current voltage characteristics (measured at STC), it is evident that the value of negative voltage potential is not directly proportional to the PID occurrence. These results are supplemented by electroluminescence images which confirm this finding.

1. Introduction

Potential Induced Degradation (PID) issue is nowadays a discussed topic through the scientific institutions around the world. The reason of the silicon-based PV cells efficiency reduction due to PID is thoroughly studied in many foreign publications [1–6,13]. Naumann et al. has described PID as the occurrence of PN junction short-circuits at the atomic level due to stacking faults at *p*-type PV cells [7]. In [7] is the sodium ions distribution on the surface of the PV cell examined in detail. A summarizing article was published in [8]. Further explanation of PID degradation of n-type PV cells is due to the increased front surface recombination velocity that is examined by groups of scientists in publications [14,15]. All publications dealing with the PID degradation confirm that the PID origin is related to the high voltage potential between the aluminum frame and the PV module cells. One of the reasons is the connection of many FV modules in series. From the laboratory experiments it was found that the magnitude of the voltage potential, degradation time and environmental conditions such as temperature and humidity affect the extent of the PID in PV modules [9,10,13].

The occurrence of PID degradation on the real PV power plants is gradual and takes many years until it becomes fully apparent. This is because of environmental conditions which accelerate the PID degradation as well as due to vulnerability of PV cells in PV modules. The incubation time cannot be estimated precisely and it depends on the location and conditions in which the PV power plant is operated. One of the reason which leads to the degradation process beginning is the power plant design to higher power. The power plants with higher number of PV modules connected in series on the high potential between the cells and the earthed frame are more vulnerable to PID. When the so-called floating grounding string is used (the positive and also the negative pole of the string are not earthed) a negative voltage potential causes the leakage currents from the PV cells through the sandwich structure of the PV module into the grounded frame. The value of leakage currents depends on the materials used in PV modules, e.g., EVA foils [21,23]. The resulting negative electric field between the aluminum frame and the cells accelerates the movement of the positive ions from the cover glass of the PV module through the sandwich structure to the PV cells, where they can cause a decrease of efficiency [1].

The extent of PID degradation at individual PV modules should be proportional to the magnitude of the negative voltage potential due to position of the PV module in the string and also depending on the materials from which the PV module is composed (encapsulated material, type of PV cells). The individual PV module layers can also play a large role in the PID vulnerability. The PV modules consist of several parts hermetically sealed and encapsulated in an aluminum frame. Photovoltaic cells are most often encapsulated in ethylene vinyl acetate foil (EVA). The protective glass is used as the top layer for the protection of the photovoltaic cells against environmental effects. Bottom of the photovoltaic module is covered with the polyvinyl fluoride laminate (PVF). For example, in article [23] it has been proven that lamination materials used for protection and galvanic separation of photovoltaic

* Corresponding author.
E-mail address: xhylsk00@stud.feec.vutbr.cz (J. Hylský).

https://doi.org/10.1016/j.microrel.2018.04.003
Received 18 September 2017; Received in revised form 28 March 2018; Accepted 4 April 2018
Available online 11 April 2018

Table 1
Parameters of module ES - A - 205 - fa3 (measured at STC).

P_{MPP} (W)	Eff_{MIN} (%)	V_{MAX} (V)	I_{MAX} (A)	V_{OC} (V)	I_{SC} (A)
205	13.1	18.2	11.27	22.7	11.93

components can directly affect the extent of PID degradation. Replacement of the widely used ethylene vinyl acetate material by an alternative material with the slower sodium ions migration can rapidly decrease the PID degradation. One of the alternative materials is partially neutralized polyethylene commercially known as Acit [23].

Most of the scientific studies of the PID effect are investigated on laboratory-degraded PV modules and PV cells [18,19,22]. In our research are PID-damaged PV modules from a power plant that has been in operation for 7 years. For this reason, degradation effects and PID mechanisms could be fully demonstrated and understood.

2. PV power plant description

The analyzed PID affected PV power plant has an output power of 2 MWp. Power plant is equipped with 205 W and 210 W Evergreen photovoltaic modules. The basic parameters of the modules are summarized in Tables 1 and 2. This PV power station was launched in 2010.

PV power plant consists of 55 strings, marked as WR1–WR55. In each string are 32 PV modules connected to series. The sum of their voltages is close to 600 V (maximal allowed value for the string in the Czech Republic). The PV modules are located at a 45° angle to the south side. PV modules are equipped with the *p*-type silicon PV cells. The inverter is installed at the output of each string. The inverter does not contain galvanic isolation (e.g., transformer) so grounding of the negative pole of the string cannot be chosen. Without grounding the positive and negative poles of the inverter, the string split into a positive and negative part, as is described in the publication [21]. Such an arrangement is called floating potential. Since the same types of PV module with the same maximum V_{MAX} voltage parameter are used, zero potential will occur in the middle of the string.

3. PID analysis and result discussion

The thermo-vision method, as referred in [16], can be used for diagnosis of PID degradation directly at PV power plant. Using the thermo-camera images can localize the affected PV modules on the negative pole of the string. Therefore, the initial diagnosis and PID degradation verification was performed by thermo-camera FLIR E4 see Fig. 1. Fig. 1 compares some PV modules from the negative pole of the string WR14 with the PV module from the positive pole of the string WR14. Images were taken from the back of the PV module to minimize reflection of the light from the module glass.

As can be seen from the thermal images, there are degraded PV cells in the PV modules selected from the negative pole of the string whereas, the module located in the positive part of the string are without defective cells. This partly confirms the occurrence of PID degradation in the PV power plant. The same degradation phenomenon was found also on other PV modules installed in the other strings of the PV power plant.

A well distribution of affected PV cells can be seen from the PV module from the WR14 string connected to the negative voltage of 300 V, see Fig. 2. It is obvious that the degraded PV cells are not only

Table 2
Parameters of module ES - A - 210 - fa3 (measured at STC).

P_{MPP} (W)	Eff_{MIN} (%)	V_{MAX} (V)	I_{MAX} (A)	V_{OC} (V)	I_{SC} (A)
210	13.4	18.3	11.48	22.8	12.11

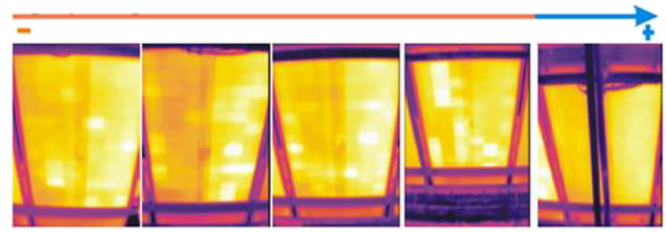

Fig. 1. Images of selected ES - A - 210 - fa3 PV modules taken by thermo-camera from the back side of WR14 string.

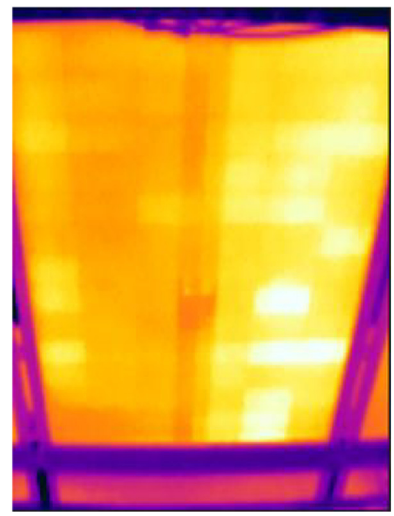

Fig. 2. Thermo-image of the PV module negative string WR14 (applied voltage potential of 300 V). Degraded PV cell in the entire surface of PV module.

along the aluminum frame but on the entire surface of the PV module. From the results of the laboratory experiments [19,22] it was concluded that the decrease in the observed PV cell parameters (open circuit voltage V_{oc}, short current I_{sc} or P_{MPP} maximum power etc.) depends on time of degradation, temperature, pressure and humidity. In our case we do not have to consider influences of environmental condition because of the same weather condition in the power plant during its lifetime. The results published in recent years have shown a direct proportion of PV cells potential induced degradation (decrease in maximum power) due to the increasing intensity of the electric field [18].

Higher values of negative voltage potential rapidly accelerate the process of PV cells degradation which helps sodium ions pass through the SiN_x antireflection layer and then create local short-circuits in the PN junction. The model of an analyzed PV module has been created in SolidWorks software for the simulation of electric field displacement, see Fig. 3. The voltage potential of −300 V was used. According to the assumption it can be seen that the highest value of electric field strength is about 150 kV m^{-1} along the PV module edges. Towards the center gradually due to increasing distance from the aluminum frame to the middle of PV module value of the electric field strength has dropped to the value of 1.6 kV m^{-1}. According to comparison of the thermal images of Fig. 2 and the electric field displacement in Fig. 3 we can conclude that the value of the electric field strength is not always directly proportional to the extent of degradation of individual cells in the PV modules.

This model was simulated for the common state of the PV module when there was not conductivity of the surface glass. There are therefore no impurities on the surface that can increase its conductivity.

These results differ from the findings of publication [17] where PV cells affected by PID degradation are predominantly at the edges of the PV module. Therefore, the generally accepted statement that most of

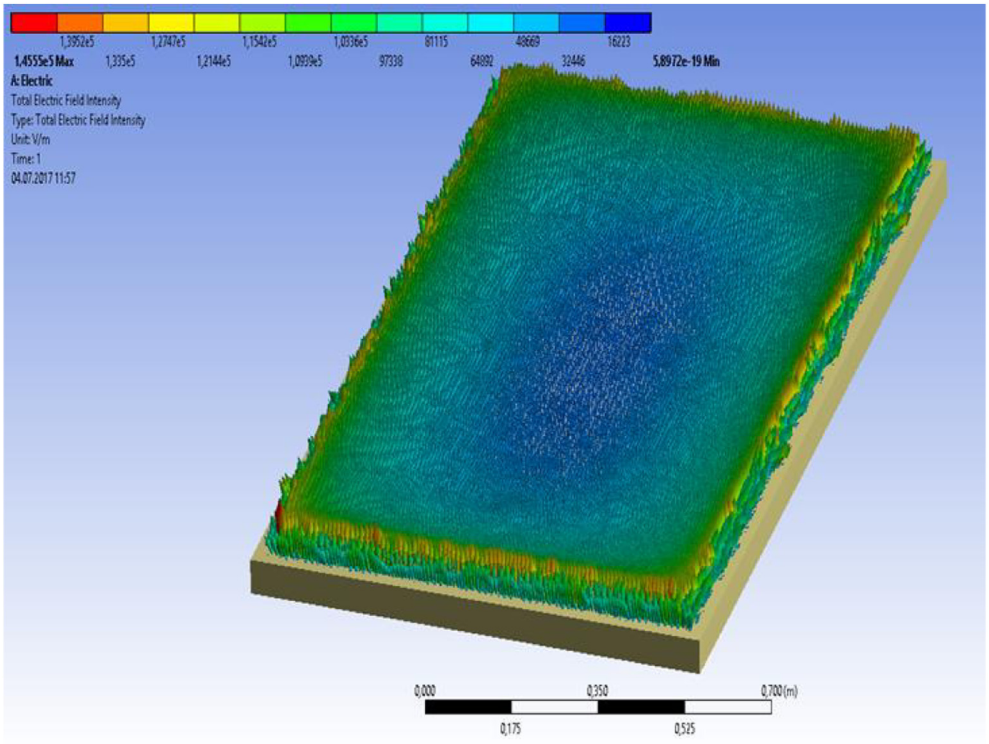

Fig. 3. Simulation of the electric field strength on the PV module surface (applied voltage potential of −300 V).

the PID-affected PV modules reducing output power in the PV power plant string are at the highest negative potential is wrong. It can be concluded that it does not depend only on the magnitude of the electric field intensity but also on the PV cells themselves and their sensitivity to PID degradation. There is a question how much negative potential causes the PID processes.

According to the publications [17,20] describing the affected power station by PID degradation and also laboratory results [21,22] the most affected PV modules occur at the highest negative pole of the string. By gradual voltage increasing to the positive values, the PID degradation should be lost. In the next part of this article the extent of degradation of individual PV modules in the negative part of the WR14 string is analyzed and differs rapidly from the expected results published in [17,20].

Fig. 4 shows dependencies of PV modules positions in WR14 string to voltage potential. Position number 1 indicates PV module location in the most negative part of the string where the value of the negative potential to ground is around −310 V. The value of the voltage on the next position of the PV module No. 2 can be calculated as $-310 + V_{MAX}$. V_{MAX} is the value of the maximum PV module voltage specified by the manufacturer, see Table 2. The negative potential of each subsequent PV module positions decreases by the V_{MAX} up to the zero potential corresponding to position 18. From this position is on the photovoltaic modules applied positive voltage potential corresponding to $0 + V_{MAX}$ for the position 19. As mentioned in the description of the PV power plant the string is divided into negative and positive part due to the ungrounded poles (floating grounding).

For a comparison of the extent of the PID on the individual PV

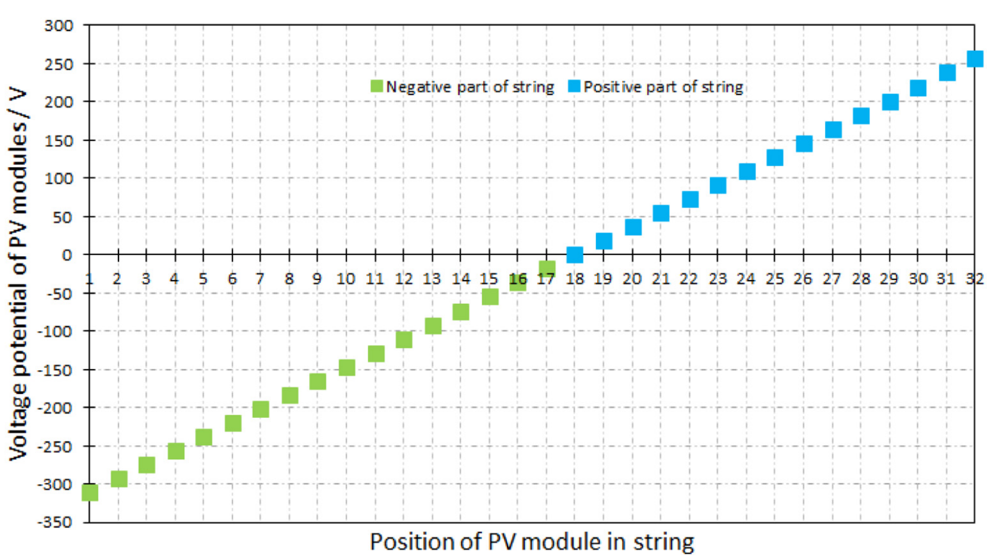

Fig. 4. Voltage potential vs. PV modules positions in WR14 string.

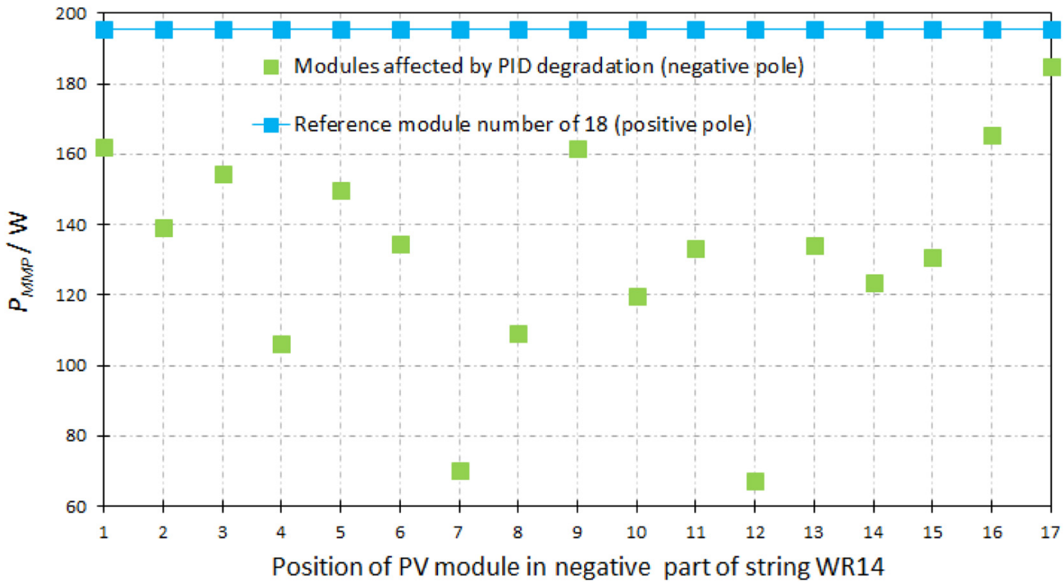

Fig. 5. The maximum power point P_{MPP} values of the individual PV modules located in the negative part of the WR14 string (1–17) compared to the reference PV module No. 18 value P_{MPP} (measured at STC).

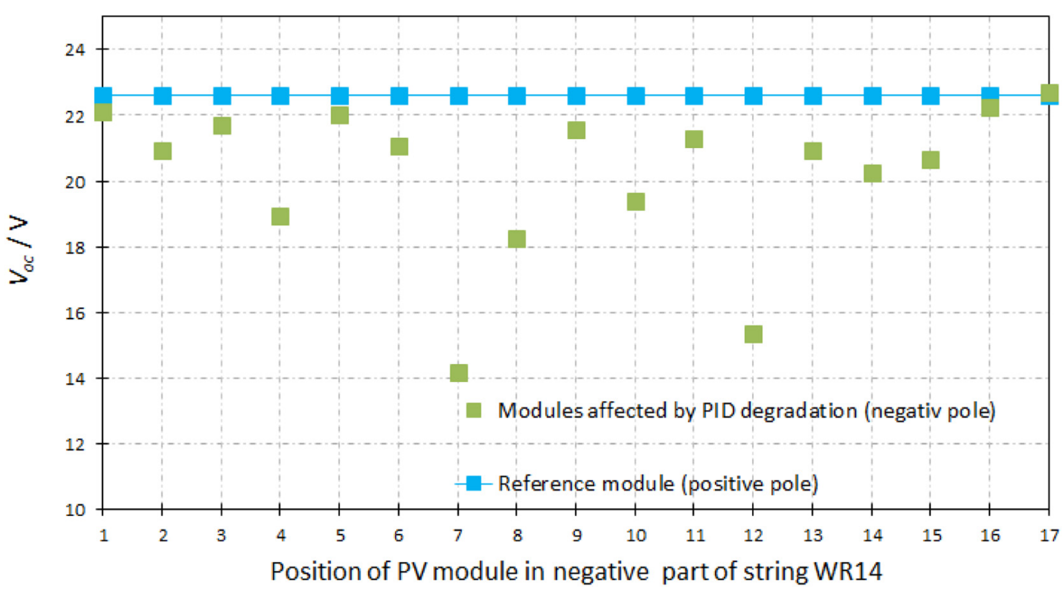

Fig. 6. Open circuit voltage values V_{OC} of individual PV modules located in the negative part of string WR14 (1–17) compared to reference PV module No. 18 value V_{OC} (measured at STC).

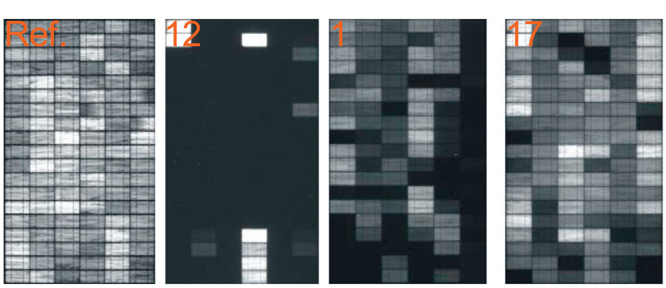

Fig. 7. PV module electroluminescence images for individual positions in the string (Reference module position 18 = without PID, position 12/ −110 V = extensive PID, position 1/−310 = PID degradation of some PV cells, position 17/−20 V = only a few degraded PV cells).

modules has been chosen one from the position 18 as a reference model because there is no effect of negative voltage potential and no observation of the PID. For an evaluation were chosen two parameters: value of the maximum power P_{MPP} and open circuit voltage V_{OC}. PV modules from the negative pole of WR14 WR14 were dismantled and measured in the accredited laboratory of Brno University of Technology. PASAN Sun Sim 3C flash tester has been used to maintain STC conditions. Following Figs. 5 and 6 show the maximum values of P_{MPP} power and V_{OC} voltage of the individual PV modules.

The measured values of the P_{MPP} and V_{OC} cannot be interpreted by any mathematically function or defined as an increasing or decreasing dependencies. Therefore, the generally accepted statement that most of the PID-affected PV modules reducing output power in the PV power plant string are at the highest negative potential is wrong. The comparison of position 12 shows one of the largest differences between P_{MPP} and V_{OC} from the reference PV module at positon 18 while the negative voltage potential is only −110 V.

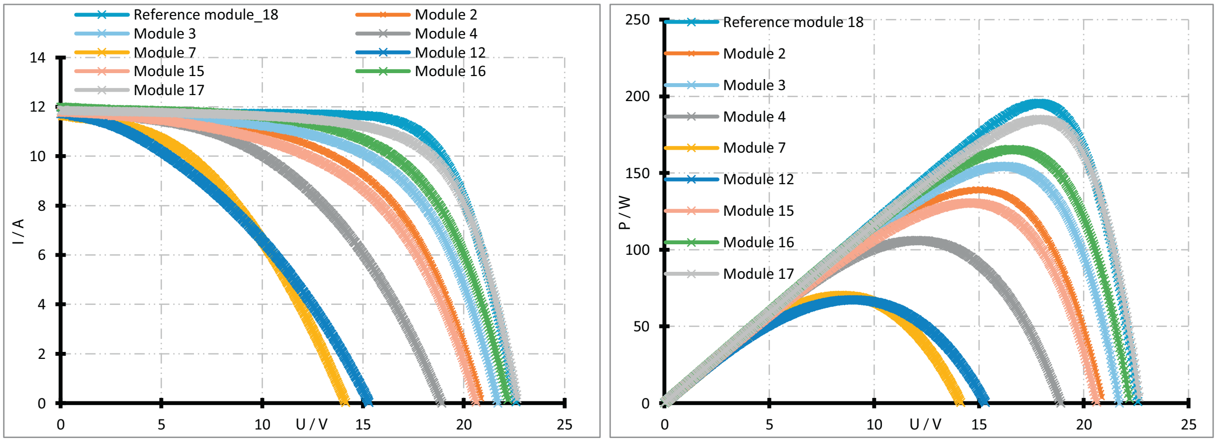

Fig. 8. IV characteristics (left) and performance characteristics (right) of selected PV modules from the WR14 string.

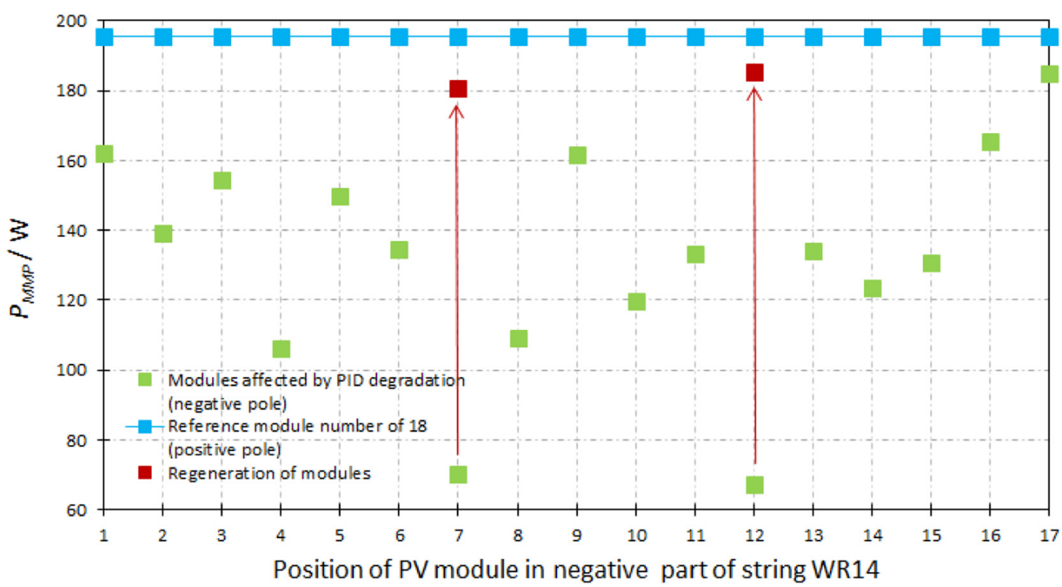

Fig. 9. Maximum power point values of individual PV modules located in the negative part of string WR14 (1–17) compared to the reference value PV module No. 18 and with regenerated PV modules at positions 7 and 12 (Measured at STC).

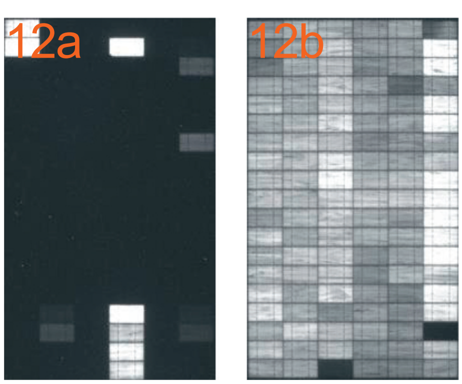

Fig. 10. Electroluminescence images of PV modules on position 12. 12a) PV module before and 12b) after the regeneration process.

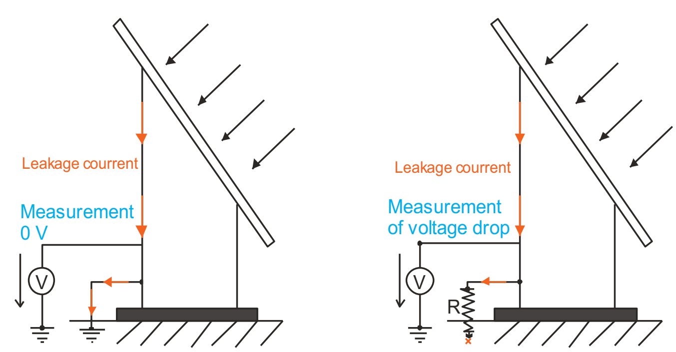

Fig. 11. Illustrative illustration of the correct (left picture) and faulty grounding (right picture) of the PV module frame and the supporting structure.

Fig. 7 compares the PV modules images taken by an electroluminescence measurement, where the extent of degradation correlates with the measured values of the P_{MPP} and V_{OC} parameters at the appropriate positions of the PV modules. PID degraded PV cells contain short circuits in the PN junction which do not allow generation of electron - hole pairs. Subsequent radiant recombination cannot be captured on the CCD camera. Therefore, degraded PV cells are displayed as black due to electroluminescence measurement. For the electroluminescence measurement was used a DC Diametral R124R50E source and a G2CCD CCD camera.

The results are complemented by the IV characteristics and performance characteristics of selected PV modules from the WR14 string. From these dependencies in Fig. 8 are noticeable changes of the individual parameters of the PV module, such as V_{OC}, I_{SC} and R_{SH}, due to PID degradation.

The question here is whether the PV modules at positions 7 and 12 are not burdened with other degradation mechanisms or if they are not mechanically damaged. As confirmed by the publication [13], PID degradation is a reversible process. Using the opposite electric field than occurs in PID degradation, the out-diffusion of sodium ions from stacking faults occurs and also dispersion of sodium ions to the antireflection coating layer of silicon nitride. This process re-closes the short circuits and increase the value of the PV cells shunt resistance R_{SH}. The regeneration process itself accelerates the increase of temperature, which results in an increased mobility of sodium ions in SiO_2 and in silicon nitride SiN_x [13]. In PV modules at positions 7 and 12, regeneration was performed using reversed electric field with a 600 V positive voltage between the terminals and the aluminum frame of the PV module for 240 h. The ambient temperature was 24 °C and was therefore not increased so the regeneration process was not accelerated. The relative humidity of the laboratory rooms was 30%. Maximum power point P_{MPP} parameter of regenerated PV modules is shown in the graph in Fig. 9.

Fig. 9 shows the large regenerative capability of PV modules due to the inverted electric field with a positive voltage of 600 V. It can be assumed that PV modules are only affected by PID degradation without any other defects. A slight difference in maximum power point between reference and regenerated modules could occur due to incomplete regeneration or due to irreversible PID degradation of the PV cells. This is illustrated by Fig. 10, including the electroluminescence images of the PV module at position 12, before and after the regeneration process. In Fig. 10b are visible regenerated solar cells except those who may have already irreversible degradation level, or with the longer regeneration period was needed.

PID doctors work on this regeneration principle in a real working condition of the PV power plants. These regenerative systems are installed in the individual string inverters. In cases where the PV power does not generate electrical energy, this system returns between the PV module frame and its potential reverse polarity. The electric field of the inverted direction and the separation of the sodium ions from the layer errors are created. As a result, PN transition short circuits will disappear. This option of PV power plant healing prolongs the PV system versatility due to the high purchase price of the PID doctors.

The possibility of poor connection and grounding of the string construction with the aluminum frames of the individual PV modules was also analyzed. In the case of a grounding failure, different negative voltage potential could affect the individual PV modules, which could lead to an unproportional potential induced degradation in comparison with the negative voltage values, see Fig. 11. However, measuring the voltage potential between the newly created grounded pin and the individual frames of the PV module has rejected this option.

PID is accelerated by environmental influences, especially humidity and temperature [5,10–12,22]. Taking into account the same conditions for all PV modules connected in the WR14 string, the effect of the temperature can be neglected. The moisture penetration into the sandwich structure of specific PV modules is possible in the event of a faulty seal isolation around the PV module. Thus can increased the leakage currents and speeding up the PID degradation itself. This would explain the large extent of PID degradation in PV modules at positions 7 and 12. However, after thorough examination of the PV modules at positions 7 and 12, no signs of encapsulation disruption or delamination of EVA foil, discoloration of EVA foil and corroded interconnection contacts between PV cells were found. Considering that all PV modules in the string are made from the same materials, these results may lead to the conclusion that the PV module degradation is dependent on PV cells and their susceptibility to PID. The question is what negative voltage potential can cause PID degradation in PV modules with PID prone PV cells. This idea is the goal of further measurement and research.

4. Conclusion

In this paper, a 2 MW PV power plant was analyzed. The first step of the analysis was to scan the PV plant panels using a thermal camera. The resulting images confirm that photovoltaic modules are infected with PID. From the thermal images of the affected PV module, it was clear that the degraded PV cells are not only along the aluminum frame but randomly distributed over the entire surface of the PV module. From the PV module electric field intensity simulation was determined values of intensity of individual PV cells. These results show that potential induced degradation of photovoltaic cells, modules is not proportional to the magnitude of the negative potential. On the contrary, it depends on the specific susceptibility to PID degradation of the individual PV cells structures. Furthermore, the volt ampere characteristics of the PV modules from the negative pole of the selected string WR14 were measured. The maximum power point parameters P_{MPP} and open voltage circuits V_{OC} were selected as PID range indicators. These values also showed that the extent of degradation of individual PV modules is not proportional to the magnitude of the negative voltage potential. To confirm that the PV module performance drop is only caused by PID degradation, the most affected cells have been regenerated with the inverted polarity voltage. These measurements are supplemented with electroluminescence images. Even these results suggest that the extent of degradation of the PV module is dependent on the installed PV cells and their susceptibility to PID degradation - more precisely about occurrence of structural defects such as slight scratches on the Si surface of PV cell, where stacking faults can grow (under the influence of PID stress) and subsequent local short-circuit of PN junction may appear.

Acknowledgments

This research has been carried out in the Centre for Research and Utilization of Renewable Energy (CVVOZE). Authors gratefully acknowledge the financial support from the Ministry of Education, Youth and Sports of the Czech Republic under NPU I programme (project No. LO1210).

References

[1] J. Bauer, V. Naumann, S. Großer, C. Hagendorf, M. Schütze, O. Breitenstein, On the mechanism of potential-induced degradation in crystalline silicon solar cells, Phys. Stat. Solidi (RRL) Rapid Res. Lett. 6 (8) (2012) 331–333.
[2] V. Naumann, C. Hagendorf, S. Grosser, M. Werner, J. Bagdahn, Micro structural root cause analysis of potential induced degradation in c-Si solar cells, Energy Procedia 27 (2012) 1–6.
[3] V. Naumann, D. Lausch, S. Großer, M. Werner, S. Swatek, C. Hagendorf, J. Bagdahn, Microstructural analysis of crystal defects leading to potential-induced degradation (PID) of Si solar cells, Energy Procedia 33 (2013) 76–83.
[4] V. Naumann, D. Lausch, A. Hähnel, J. Bauer, O. Breitenstein, A. Graff, M. Werner, S. Swatek, S. Großer, J. Bagdahn, C. Hagendorf, Explanation of potential-induced degradation of the shunting type by Na decoration of stacking faults in Si solar cells, Sol. Energy Mater. Sol. Cells 120 (2014) 383–389.
[5] V. Naumann, D. Lausch, A. Hähnel, O. Breitenstein, C. Hagendorf, Nanoscopic studies of 2D-extended defects in silicon that cause shunting of Si-solar cells, Phys. Status Solidi C 12 (8) (2015) 1103–1107.
[6] V. Naumann, C. Brzuska, M. Werner, S. Großer, C. Hagendorf, Investigations on the formation of stacking fault-like PID-shunts, Energy Procedia 92 (2016) 569–575.
[7] S.P. Harvey, J.A. Aguiar, P. Hacke, H. Guthrey, S. Johnston, M. Al-Jassim, Sodium accumulation at potential-induced degradation shunted areas in polycrystalline silicon modules, IEEE J. Photovolt. 6 (6) (2016) 1440–1445.
[8] W. Luo, Y.S. Khoo, P. Hacke, V. Naumann, D. Lausch, S.P. Harvey, J.P. Singh, J. Chai, Y. Wang, A.G. Aberle, S. Ramakrishna, Potential-induced degradation in photovoltaic modules: a critical review, Energy Environ. Sci. 10 (1) (2017) 43–68.
[9] S. Hoffmann, M. Koehl, Effect of humidity and temperature on the potential-induced degradation, Prog. Photovolt. Res. Appl. 22 (2) (2014) 173–179.
[10] H.-C. Liu, C.-T. Huang, W.-K. Lee, M.-H. Lin, High voltage stress impact on P type crystalline silicon PV module, Energy Power Eng. 05 (07) (2013) 455–458.
[11] M. Koehl, S. Hoffmann, Impact of rain and soiling on potential induced degradation, Prog. Photovolt. Res. Appl. 24 (10) (2016) 1304–1309.
[12] P. Hacke, K. Terwilliger, R. Smith, S. Glick, J. Pankow, M. Kempe, S.K.I. Bennett, M. Kloos, System voltage potential-induced degradation mechanisms in PV modules and methods for test, 2011 37th IEEE Photovoltaic Specialists Conference, 2011, pp.

000814–000820.
[13] D. Lausch, V. Naumann, A. Graff, A. Hähnel, O. Breitenstein, C. Hagendorf, J. Bagdahn, Sodium outdiffusion from stacking faults as root cause for the recovery process of potential-induced degradation (PID), Energy Procedia 55 (2014) 486–493.
[14] R. Swanson, M. Cudzinovic, D. DeCeuster, V. Desai, J. Jürgens, N. Kaminar, W. Mulligan, L.R. Barbosa, D. Rose, D. Smith, A. Terao, K. Wilson, The surface polarization effect in high - efficiency silicon solar cells, Proceedings of 15th International Photovoltaic Science and Engineering Conference (PVSEC-15), Shanghai, China, 2005.
[15] K. Hara, K. Ogawa, Y. Okabayashi, H. Matsuzaki, A. Masuda, Influence of surface structure of n-type single-crystalline Si solar cells on potential-induced degradation, Sol. Energy Mater. Sol. Cells 166 (2017) 132–139.
[16] T. Kaden, K. Lammers, H.J. Möller, Power loss prognosis from thermographic images of PID affected silicon solar modules, Sol. Energy Mater. Sol. Cells 142 (2015) 24–28.
[17] H. Yang, F. Wang, H. Wang, J. Chang, D. Song, C. Su, Performance deterioration of p-type single crystalline silicon solar modules affected by potential induced degradation in photovoltaic power plant, Microelectron. Reliab. 72 (2017) 18–23.
[18] M. Barbato, A. Barbato, M. Meneghini, G. Tavernaro, M. Rossetto, G. Meneghesso, Potential induced degradation of N-type bifacial silicon solar cells: an investigation based on electrical and optical measurements, Sol. Energy Mater. Sol. Cells 168 (2017) 51–61.
[19] S. Yamaguchi, K. Ohdaira, Degradation behavior of crystalline silicon solar cells in a cell-level potential-induced degradation test, Sol. Energy 155 (2017) 739–744.
[20] J. Chang, H. Wang, H. Yang, J. Zhang, J. Huang, The real situation of potential-induced degradation in multicrystalline silicon photovoltaic power plant, 2016 IEEE 43rd Photovoltaic Specialists Conference (PVSC), 2016, pp. 1682–1685.
[21] S. Pingel, O. Frank, M. Winkler, S. Daryan, T. Geipel, H. Hoehne, J. Berghold, Potential induced degradation of solar cells and panels, 2010 35th IEEE Photovoltaic Specialists Conference, 2010, pp. 002817–002822.
[22] A. Masuda, M. Akitomi, M. Inoue, K. Okuwaki, A. Okugawa, K. Ueno, T. Yamazaki, K. Hara, Microscopic aspects of potential-induced degradation phenomena and their recovery processes for p-type crystalline Si photovoltaic modules, Curr. Appl. Phys. 16 (12) (2016) 1659–1665.
[23] J. Kapur, K.M. Stika, C.S. Westphal, J.L. Norwood, B. Hamzavytehrany, Prevention of potential-induced degradation with thin Ionomer film, IEEE J. Photovolt. 5 (1) (2015) 219–223.